Recycling of the Flue Gas from Aluminium Electrolysis Cells

Asbjørn Solheim and Samuel Senanu

SINTEF, P.O. Box 4760 Torgarden, NO-7465 Trondheim, Norway

Key words: Flue gas, Recycling, Gas composition, Heat recovery

Abstract

Recycling of the flue gas from aluminium reduction cells is a possible method for increasing the CO_2 concentration, thereby enabling CO_2 capture. The present paper represents a preliminary study concerning some of the consequences in the electrolysis cells. The energy balance in a hypothetic 400 kA cell was estimated, and it turned out that the heat flow into the superstructure could be kept constant by decreasing the thickness of the anode cover material even with a very hot gas. Recycling gives a higher amount of collectible heat from the cells, mainly because of higher temperature in the gas entering the cell. It will be advantageous to apply catalytic burning of CO to CO_2, which represents considerable extra heat. Increased sulfuric acid dewpoint may represent a challenge. It is also necessary to address the amount of hydrogen fluoride that re-evolves from the secondary alumina at high superstructure temperature.

Introduction

Recycling of the flue gas from aluminium electrolysis cells has been patented by General Electric [1, 2]. The main idea is to cool down at least some of the gas withdrawn from the cell and recycle it, thereby reducing the use of ambient air. The idea has not been realised in an industrial setting, and as far as the authors are aware, the idea has not yet been thoroughly discussed or analysed in the open aluminium society. Recycling has some indisputable advances, which will be particularly important in a future scenario where low carbon dioxide emissions and utilisation of surplus heat are considered more important than today. Some of the potential benefits, as summarised in the patents, are:

- The flue gas volume will be considerably reduced. This means that ducts and gas treatment centres (GTCs) can be made much more compact, saving CAPEX as well as OPEX.
- The flue gas will be more concentrated in dust, hydrogen fluoride, sulfur dioxide, and carbon dioxide. This simplifies gas scrubbing, and it will be easier to construct an efficient CO_2 removal device.
- Smaller amounts of water vapour contained in the ambient air will be transported through the system, which will reduce scaling. Therefore, it will be easier to operate process equipment such as heat exchangers.
- The cooled gas recycled to the cell can be used for protecting vital equipment inside the hood.
- The cooled recycled gas can also be supplied to form a "curtain" around the alumina feeders, thereby reducing the amount of alumina dusting.

There may also be other advantages that are not mentioned in the patents. The fluoride concentration in the secondary alumina may be higher, which means that a part of the plant can be operated with virgin alumina, giving high purity metal. There will be also be more heat available in the flue gas, and lower concentration of oxygen inside the superstructure will probably reduce airburn of the anodes.

However, there are also some potential challenges that must be considered. The most obvious objection to the idea is that the cell superstructure must be considerably tighter than today. Still, the superstructure must be opened for setting of new anodes. Recycling of gas may require many units (high CAPEX), although it will be possible to serve several neighbouring cells with the same set of fan and heat exchanger. There may also be challenges related to higher concentrations of harmful gases, such as HF, CO, and SO_2.

The purpose of the present report is to deliver a preliminary analysis concerning the cell energy balance, the heat available in the flue gas, and the gas composition in a cell with recycled gas. Finding practical solutions is not a part of the current treatment.

Recycling: Main Idea

In the normal situation, all gas evolved underneath the anode and the air sucked into the cell is transferred directly to the gas treatment centre through ducts that may be several hundred meters long. A very high surplus of air is used, so the content of gases produced in the cell is typically about 1 percent. The flue gas represents the largest mass flow in the process, with up to 100 t gas/t Al.

The reason for having such a high gas flow is twofold; it is necessary to have sufficient underpressure inside the superstructure to avoid fluorides entering the potroom, and it is necessary to cool the gas to protect equipment at and inside the superstructure. The same effects can, however, be achieved by recycling the gas and cooling it in a heat exchanger (HEX) before it is returned to the cell, as illustrated in Figure 2.1. The total gas flow G_{out} in the figure can be about the same as in today's practice, while fan power can be saved because the gas flow to the GTC can be reduced.

In Figure 1 as well as in the subsequent treatment, it was assumed that there is one fan and HEX for each electrolysis cell. However, it may be sensible to treat several neighbouring cells with the same set of fan and HEX. This will require fewer pieces of equipment and probably less CAPEX, but the pressure drop in the recirculation loop may be higher.

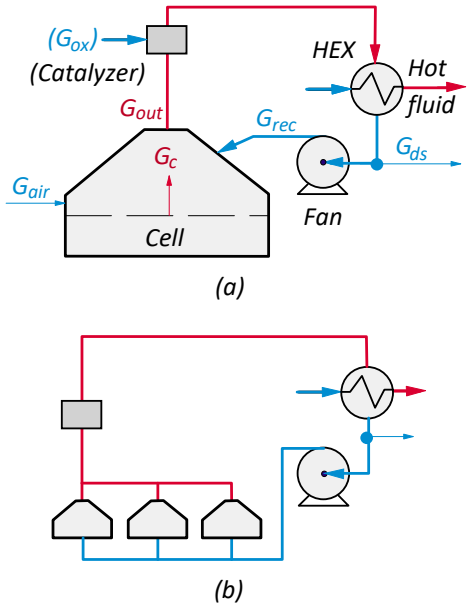

Figure 1. a): Principal sketch of an aluminium electrolysis cell with gas recycling. G_{air}: Air sucked into the cell superstructure from the outside, G_c: Gas evolved in the cell reactions, G_{out}: Gas extracted from the cell, G_{ox}: Air or oxygen supplied to catalytic burner for oxidizing CO to CO_2, G_{rec}: Gas recycled to the cell, G_{ds}: Gas to the dry scrubber. b): Several cells may be served by one fan and HEX.

Basis for the Calculations

Main Cell Data

A modified version of the pragmatic aluminium cell model used by Ladam et al. [3] was employed in the current work. The model comprises the cell and its superstructure. Although strongly simplified, all known couplings in the process are accounted for in the model. The data predicted generally comply reasonably well with measurements in industrial cells and data obtained from other models.

All results in the present work relate to a hypothetical modern 400 kA cell with 40 prebaked anodes. The cell voltage was assumed to be 4.05 V, corresponding to a DC energy consumption of 12.77 kWh/kg Al at 94.49 percent current efficiency. At normal conditions (draught 10 000 Nm^3h^{-1}, without recycling), there was ample sideledge and the superheat was reasonable (5.4 °C), while the average anode-cathode distance was estimated to be 31 mm. The temperature of the gas inside the superstructure was 138 °C. The heat needed to bring a newly set anode up to service temperature is included in the reaction enthalpy, and "smeared out" over its service time.

Energy Balance for the Superstructure

Figure 2 illustrates the effect of the draught (G_{out}, see Figure 1) on the cell and superstructure heat balance. As would be expected, lower draught gives higher temperature inside the superstructure and, thereby, lower heat flow through the anode and crust, which in its turn leads to decreased ledge thickness, higher superheat, and lower current efficiency. It is, however, in most cases, possible to increase the upward heat loss by decreasing the thickness of the anode cover material to retain the energy balance at the top of the cell. (An exception may be the situation where the cell is running at the upper part of its operational window, *i.e.*, at its maximum amperage, where the bottleneck is the capacity of transporting heat from the interior of the cell). In the present case, it was found that a draught of 10 000 Nm^3h^{-1} with 15 cm thickness of the anode cover material (ACM) produced the same upwards heat loss as 1000 Nm^3h^{-1} draught with 5 cm ACM. The relatively weak dependence between draught (or temperature) and heat loss is supported by a recent work by Arkhipov et al. [4]. For operation at the lowest possible energy consumption, high superstructure temperature is an advantage insofar as at it lowers the heat loss. The thin lines in Figure 2 represent the case where the heat loss from the interior of the cell was kept constant (same value as with 10 000 Nm^3h^{-1}).

It was assumed that 50 percent of the carbon monoxide generated underneath the crust was oxidised to carbon dioxide. This was based on the observation that the CO/CO_2 ratio appears to be about 0.1 [5]. The enthalpy for oxidation of CO to CO_2 is nearly constant in the temperature range 300-800 K, $\Delta H^0 = -283.4 \pm 0.3$ $kJmol^{-1}$ [6]. The heat of burning CO represents an added heat source of approximately 30 kW inside the superstructure.

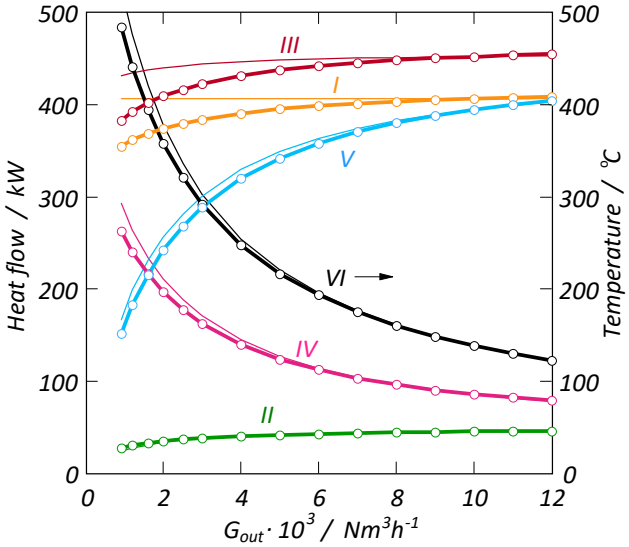

Figure 2. Temperature and heat flows as a function of the draught in a 400 kA cell. Curve I: Heat conducted into the superstructure from the interior of the cell (including radiation from open feeder holes and heat from burning CO), and ohmic heat generated in the anode assembly; Curve II: Enthalpy released by cooling of hot anode gas to the superstructure temperature; Curve III: Total heat into superstructure (sum of I and II), Curve IV: Heat loss from the superstructure; Curve V: Heating of ambient air from 30 °C; Curve VI: Gas temperature in superstructure. Thin lines: Fixed heat loss from the interior of the cell (same value as with G_{out} = 10 000 Nm^3h^{-1}).

Gas Evolving Reactions

Main Cell Reaction and Parasitic side Reaction

As has been explained elsewhere, the turnover in an aluminium electrolysis cell can be written [7]:

$$\frac{\varepsilon}{2}Al_2O_3 + \frac{3}{4}C = \varepsilon Al + \frac{3}{4}(2\varepsilon - 1)CO_2 + \frac{3}{2}(1-\varepsilon)CO \qquad (1)$$

where ε is the fractional current efficiency (e.g., ε = 0.94).

It should be noted that the sum of CO and CO_2 is always ¾ moles per 3 Faraday. The relationship between current efficiency and gas composition can then be easily found from Equation 1:

$$\%CO_2 = 200\varepsilon - 100 \quad \text{and} \quad \%CO = 200 - 200\varepsilon \tag{2}$$

Equation 2 is the famous Pearson-Waddington equation, first derived in 1947 [8]. The molar flows (n) of CO_2 and CO due to the turnover reaction 1 can be calculated from Faraday's law and Equation 2,

$$n_{CO_2} = \frac{I \cdot (2\varepsilon - 1)}{4F} \quad \text{and} \quad n_{CO} = \frac{I \cdot (2 - 2\varepsilon)}{4F} \qquad [\text{mol s}^{-1}] \tag{3}$$

where I is the amperage and F is Faraday's constant [96 485 $Asmol^{-1}$].

According to Equation 2, it is possible to calculate the current efficiency from the gas composition. The method has been used in the laboratory as well as in industrial cells, but the current efficiency will be underestimated because the amount of CO_2 and CO will also be influenced by side reactions leading to excess carbon consumption.

Excess Carbon Consumption

Airburn. Carbon is thermodynamically unstable in air at all temperatures:

$$C + O_2 = CO_2 \tag{4}$$

Fortunately, oxidation is kinetically impeded below approximately 400 °C. However, the anode temperature may be much higher than this, so the anode needs to be covered with a protective ACM which is made from crushed electrolyte and alumina. The extent of airburn depends on the quality of the anode as well as the quality of the ACM application. In the present work, it was assumed that airburn accounts for 25 kg C/t Al at normal conditions (draught 10 000 Nm^3h^{-1}).

Boudouard Reaction. The Boudouard reaction can be written:

$$C + CO_2 = 2CO \tag{5}$$

CO is the thermodynamically favoured substance at cell temperature, so reaction 5 will proceed towards right as far as the relatively slow kinetics allow. The reaction takes place mainly in pores at the underside of the anode. The extent was taken to be 15 kg C/t Al in the present case.

Depending on the quality of the anode, carbon particles will fall off and end up in the bath, making "carbon froth" in extreme cases. It was assumed that the carbon particles normally are removed by the Boudouard reaction. The extent was taken to be 5 kg C/t Al.

With a current efficiency of 94.5 percent and the excessive carbon consumption mentioned above, the net carbon consumption becomes 397 kg/t Al. This is about state-of-the-art.

Fluoride, Water, and Sulfur

A model for fluoride evolution from aluminium cells was derived by Haupin and Kvande [9]. The model is mainly based on theoretical considerations, but it was also calibrated with plant data. The model is incorporated in the pragmatic model used in the present work, with the modification that the alumina activity data were updated [10]. The electrolyte composition in the present work was taken to be 11.5 wt% excess AlF_3, 5.0 wt% CaF_2, and 3.5 wt% Al_2O_3. According to "the SINTEF equation" [11], the liquidus temperature of this mixture is 951.9 °C. (The calculated temperature was adjusted downwards by 3 °C to account for elements not included in the equation).

Evaporation. It is well established that the main evaporation product from cryolitic melts is $NaAlF_4$ [12],

$$NaF(l) + AlF_3(s) = NaAlF_4(g) \tag{6}$$

The vapour also contains minor amounts of NaF(g), Na_2F_2(g), AlF_3(g), and Al_2F_6(g). $NaAlF_4$ solidifies forming aluminium fluoride and chiolite,

$$NaAlF_4(g) = \frac{2}{5}AlF_3(s) + \frac{1}{5}Na_5Al_3F_{14}(s) \quad (7)$$

In the Haupin-Kvande model, the vapour pressure is calculated from a semi-empirical equation based on vapour pressures measured in the laboratory, and it is assumed that the gas bubbles generated at the anode are saturated in vapour. In the present case, evaporation amounts to the loss of about 11.3 kg $NaAlF_4$/t Al.

Since $NaAlF_4$ solidifies, it is not considered being a part of the gas generated in the cell. The extent of evaporation is probably constant regardless of gas recycling and amount of gas extracted from the cells. It is possible that low gas flow leading to a concentrated gas may influence scaling, although the water vapour transport will be reduced.

Entrainment. Entrainment is the result of formation of tiny droplets caused by gas bubbles breaking at the electrolyte surface. Some of the droplets are small enough to be carried away with the anode gas. In the present case, entrainment was estimated to represent 1.4 kg electrolyte/t Al. Like the solidification products of $NaAlF_4$, entrained electrolyte was not regarded as a part of the generated gas.

Hydrolysis. Alumina always contains some moisture, which can be adsorbed on the internal surface or be present in the structure (highly porous γ-alumina is formed by flash-calcination of aluminium hydrate). Air sucked into the cells also contains water vapour. Water reacts with the melt to form hydrogen fluoride,

$$H_2O + \frac{2}{3}AlF_3 = \frac{1}{3}Al_2O_3 + 2HF(g) \quad (8)$$

Not all the water present reacts with the electrolyte. The equilibrium in Equation 8 depends on the electrolyte composition, and this is accounted for in the fluoride evolution model. In the present case, it was assumed that the alumina contains 1.2 wt% water and that the ambient air contains 1 vol% water vapour. The HF evolution was estimated to be 12.1 kg HF/t Al.

Evaporation products may also hydrolyse inside the superstructure (in crust openings):

$$H_2O(g) + \frac{2}{3}NaAlF_4(g) = \frac{2}{3}NaF + \frac{1}{3}Al_2O_3 + 2HF(g) \quad (9)$$

This type of hydrolysis does not affect the total fluoride evolution, but the ratio between solid and gaseous products will be altered. The hydrolysed part of $NaAlF_4$ is counted as a part of the produced HF; in the present case it amounted to 1.7 kg HF/t Al.

Sulfur Dioxide. Sulfur dioxide is the main sulfur-containing gas species in the flue gas. It stems from sulfur present in the anode,

$$S + O_2 = SO_2 \quad (10)$$

The sulfur content in the anode was set to 2.5 wt%. Only a part of the SO_2 generated is adsorbed in the dry scrubber. In the present case, it was assumed that 50 percent of the SO_2 is returned to the cell, which implies that the concentration in the flue gas is twice as high as indicated by the rate of generation at the anode.

Gas Species Generated and Consumed in Cell

Table 1 sums up the data given above. The sum of CO_2 and CO in the cell reaction is constant. Some oxygen is consumed in the airburn reaction and by formation of SO_2.

Table 1. Molar flow of gas species [mol s^{-1}] generated and consumed inside a hypothetic 400 kA aluminium electrolysis cell. Negative numbers represent consumption. Burning of CO to CO_2 inside the superstructure, e.g., in feeder holes, was not considered.

Source	CO_2	CO	O_2	H_2O	HF	SO_2
Main anode reaction	1.036	-	-	-	-	-
CO by loss in CE (94.69 % CE)	-0.110	0.110	-	-	-	-
Airburn of anode (25 kg C/t Al)	0.074	-	-0.074	-	-	-
Boudouard reaction at anode (15 kg C/t Al)	-0.044	0.088	-	-	-	-
Boudouard reaction in bath (5 kg C/ t Al)	-0.015	0.029	-	-	-	-
Water supplied with alumina (1.2 wt%)	-	-	-	0.044	-	-
Hydrolysis of bath (12.1 kg HF/t Al)	-	-	-	-0.011	0.021	-
Hydrolysis of $NaAlF_4$ (1.7 kg HF/t Al)	-	-	-	-0.002	0.003	-
From sulfur in the anode (2.5 wt%)	-	-0.011	-	-	0.011	
Sum	0.941	0.228	-0.085	0.041	0.024	0.011

Oxidation of CO to CO_2

As was mentioned above, only a part of the CO generated in the cell is oxidised to CO_2. This is related to the lower flammability limit (LFL) of CO. Several sources indicate LFL = 12-12.5 vol% CO, but the value decreases with increasing temperature [13]. Data compiled by Aarhaug and Ratvik [5] indicated that the CO/CO_2 ratio in the flue gas is close to 0.1, which means that about 50 percent of the CO is oxidised. To fully utilise the heat from oxidation of CO (283 kJ mol^{-1}), the system should contain a unit for catalytic oxidation, as indicated in Figure 1. Avoiding high concentrations of CO in the flue gas is also an important safety issue.

Gas Composition with Recycling

The concentration of the different gas species depends directly on the amount of air sucked into the superstructure, whether the gas is recycled or not. The purpose was to have high heat content in the flue gas, so it was assumed that all CO was oxidised to CO_2 using a stoichiometric amount of air. The calculations concerning gas composition are based on the data shown in Table 1 above. It is possible that some of the fluoride contained in the secondary alumina can be re-evolved at high superstructure temperature. This effect was not accounted for in the present treatment, however.

Figure 3 shows the concentration of the different gas species as a function of the amount of air. It was assumed that all the CO generated is oxidised to CO_2 by means of a stoichiometric amount of air (G_{ox}, Figure 1) in a separate catalytic unit. For this reason, the maximum CO_2 concentration is about 71 vol%, while there is 24 vol% N_2 + Ar in the flue gas. A similar calculation with pure oxygen instead of air for oxidation of CO gave more CO_2 and less N_2 + Ar (e.g., 93 vol% CO_2 and 0.7 vol% N_2 + Ar at G_{air} = 1 Nm^3h^{-1}).

It can be noted that the concentration of water vapour increases with decreasing air flow. This is due to release of water from the secondary alumina (not all the water is consumed by formation of HF).

A special feature is that when the air flow is below 4-5 Nm^3h^{-1}, the oxygen is consumed (it was assumed that there is enough oxygen for oxidation of sulfur to SO_2). In the lack of better information, the calculation assumed that the rate of airburn is proportional with the partial pressure of oxygen. With very low air flow the anode airburn simply stops, which can be regarded as an added benefit. The realism in this can be discussed however, since such low air flow requires an extremely gas tight cell.

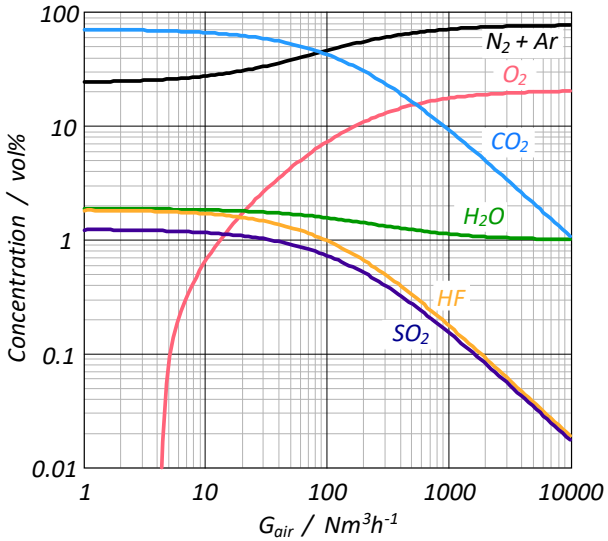

Figure 3. Concentration of gas species as a function of the air flow.

Sulfuric Acid Dew Point

In any process involving oxidation of sulfur-containing matter and the presence of humidity, aqueous sulfuric acid may be formed according to the following consecutive reactions:

$$S(s) + O_2(g) = SO_2(g) \quad (11)$$

$$SO_2(g) + \tfrac{1}{2}O_2(g) = SO_3(g) \quad (12)$$

$$SO_3(g) + H_2O(g) = H_2SO_4(g) \quad (13)$$

$$H_2SO_4(g) + x\,H_2O = H_2SO_4(aq) \quad (14)$$

The dew point is the temperature at which the first acid solution is formed according to Equation 14. The dew point is important for designing the gas treatment system and for proper materials selection. Reduced draft or recycling of gas may give a strongly concentrated gas (SO_2, Figure 3), and the HEX presents a cold surface where sulfuric acid can condense.

In aluminium electrolysis cells, the rate of formation of SO_3 from SO_2 (Equation 12) *cannot be predicted a priori,* since it is determined by kinetics as well as by thermodynamics (low temperature favours SO_3, but the kinetics are slow). The formation of SO_3 therefore depends on the oxygen supply and the thermal history of the anode gas between the anode and the area above the crust, as well as the presence of possible catalysts/inhibitors. This also implies that the effect of reduced air draught into the cells on the rate of SO_3 formation cannot be predicted. Moreover, it is possible that the SO_3 formation is different in different cell technologies or with varying bath compositions. The SO_3 concentration is usually taken to be 1-5 percent of the SO_2 concentration. These values are only relevant for flue gas from power stations, however. To our knowledge, values of the dew point in the flue gas from aluminium cells have not yet been published.

There are at least three equations available for calculating the sulfuric acid dew point, published by Okkes and Badger [14], by Verhoff and Banchero [15], and by Pierce [16]. It was decided to take the average of the three equations, since the trends in concentration dependence are similar, and the standard deviation between the equations is generally less than 10 °C. Figure 4 shows the resulting dew points as a function of the amount of air. The concentrations of water vapour and SO_2 were the same as used in Figure 3. As can be observed, the dew point may increase by up to 50 °C at very low air flow. This may, eventually, represent a material challenge.

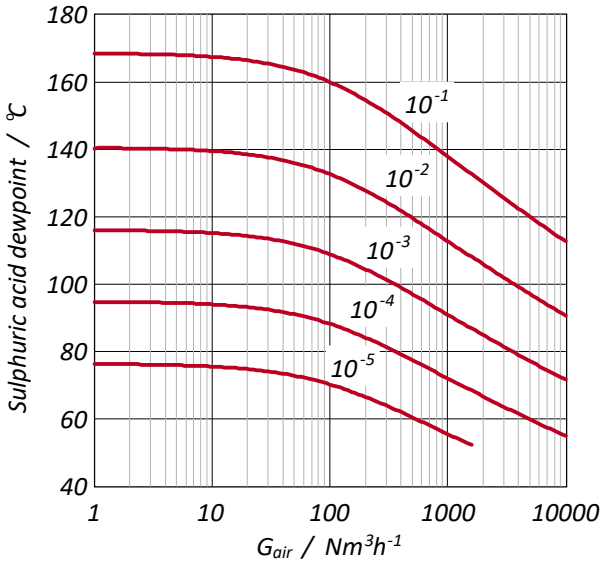

Figure 4. Sulfuric acid dew point as a function of the air draught, calculated as the average of three equations. Same gas composition as in Figure 3. The numbers in the figure represent the ratio between SO_3 and SO_2 in the flue gas. The Okkes and Badger equation is out of range at very low concentration of SO_3.

Temperature and Collectible Heat

Without Gas Recycling

The heat available for collection and utilisation was calculated under the assumption that there is no heat loss between the cell superstructure and the HEX (insulated ducts for stream G_{out} in Figure 1). The temperature of the air sucked into the cells (G_{air}) was set to 30 °C. In the cases without recycling of gas it was assumed that the ACM had constant thickness, meaning that the sideledge thickness as well the heat flow from the interior of the cell through the crust and anode decreased with decreasing air draught (see Figure 2, curve I).

The heat available in the HEX corresponds to the heat released upon cooling the flue gas from the superstructure gas temperature and down to pre-set temperatures (60, 80, 100, and 120 °C out from the HEX). The heat was calculated by using heat contents for each gas species based on linearised heat capacity data taken from NIST-JANAF [6].

The results are shown in Figure 5. As can be observed, the heat released into the HEX increases with decreasing temperature out from the HEX (but lower temperature means that it becomes more difficult to utilise the heat efficiently, particularly if a Carnot-type process is required). The available heat passes through a maximum, caused by the effects of decreasing gas temperature (to the right of the maximum) and the amount of gas available (to the left of the maximum). It should also be noted that there is a large effect of oxidation of CO, which emphasises the importance of having a unit for catalytic oxidation when the purpose is to collect heat from the flue gas.

With Gas Recycling

For calculation of available heat with gas recycling, the gas compositions shown in Figure 3 were used. The results with two conditions are shown in Figure 6. As in the previous section, the heat released upon cooling the flue gas from the superstructure temperature and down to a pre-set temperature was calculated. It was assumed that the ambient air (G_{air}) had a temperature of 30 °C, while the recycled gas (G_{rec}) had the same temperature as the temperature out from the HEX (60, 80, 100, or 120 °C). As can be observed by comparing Figs. 6 a) and 6 b), there are relatively small differences with different amounts of air (G_{air}). A smaller amount of air, i.e., smaller total gas amount and colder incoming gas, is counteracted by larger concentrations of CO_2 which has a higher specific heat capacity.

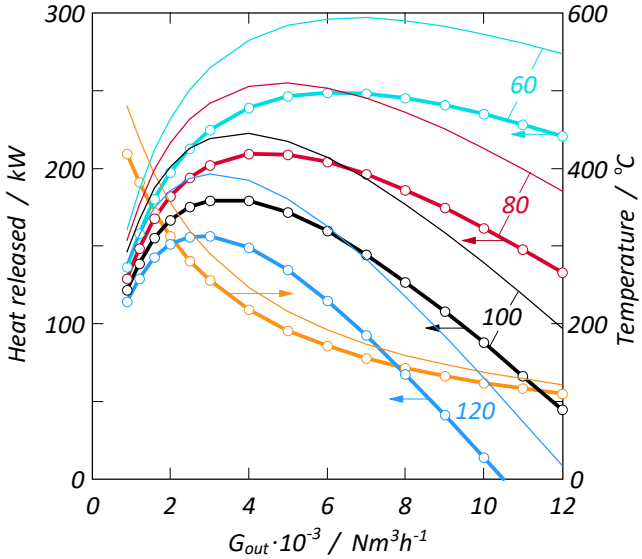

Figure 5. Temperature above crust and heat released by cooling the flue gas down to the temperatures indicated in the figure. Thick lines: Heat from oxidation of CO to CO_2 is not accounted for, thin lines: Full utilisation of the heat from oxidation of CO to CO_2.

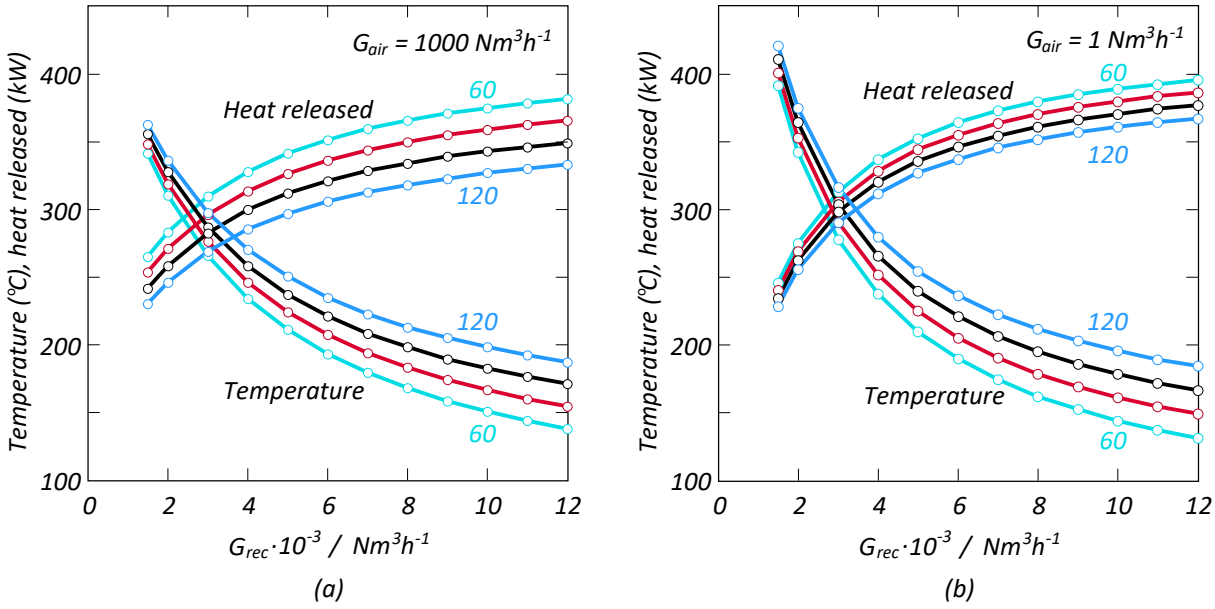

Figure 6. Temperature above the crust and heat released by cooling the flue gas down to the temperatures indicated in the figure as a function of the amount of recycled gas. Calculated with different amounts of air, a): 1000 Nm^3h^{-1}, b): 1 Nm^3h^{-1}.

Discussion

The main advantage with flue gas recycling is that it enables carbon dioxide capture. In the current practice, the CO_2 concentration is typically below one percent. The concentration can probably be increased to 3-4 percent by using distributed pot suction [17], but still, this is too low. Flue gas recycling has no principal upper limit for the CO_2 concentration (apart from the fact that it will be mixed with the other gas species generated inside the cells), so it has the potential of becoming an enabling technology in CO_2 capture from aluminium electrolysis cells. Since CO_2 has higher heat capacity than diatomic gases, the gas flow per kW heat removed from the superstructure will be smaller.

As is obvious when comparing Figs. 5 and 6, there will be more heat available for recovery if the gas is recycled. By cooling the gas down to 80 °C, the maximum heat released is 220-260 kW without recycling (depending on how much CO is oxidised to CO_2) and up to 380 kW with recycling. The main reason for the difference is that the incoming gas (G_{rec}) has a higher temperature than "fresh air" (G_{air}).

The concentrated gas can give easier scrubbing as indicated in the GE patents [1, 2], but there are also potential problems. The sulfuric acid dewpoint should be studied experimentally. Although challenging, it may be possible to use a carefully temperature-controlled mirror [18]. This can be done in existing smelters, since when the dewpoints in a few "normal" situations have been established, it will be possible to use the equations for estimating the effect of gas concentrations. This requires, however, that the oxidation of SO_2 to SO_3 is not influenced by the recycling. Higher temperature and possibly higher fluoride concentration in the secondary alumina may also represent a challenge, as fluoride will re-evolve if the temperature becomes too high.

The most important practical challenge will be to construct a tight enough superstructure that allows metal tapping and change of anodes without releasing harmful substances into the working atmosphere. One possible solution is to design the recycle loop in such a way that "forced suction" can be realised, without using a large and expensive ductwork. There will also be HES issues related to the concentrated gas. It seems that realisation of gas recycling requires that the existing methods for gas scrubbing and heat collection must be reconsidered, in the sense that it may require that the highly centralised GTCs serving typically 100 cells is replaced by more distributed systems.

References

1. G. Wedde: A Method of Ventilating an Aluminium Production Electrolytic Cell, *European Patent EP 2 360 296 A1* (2011), *US Patent US 9 458 545 B2* (2016), *US Patent US 9 771 660 B2* (2017).
2. G. Wedde, O.E. Bjarnø, and A.K. Sørhuus: Recycled Pot Gas Distribution, *US Patent US 9 234 286 B2* (2016).
3. Y. Ladam, A. Solheim, M. Segatz, and O.-A. Lorentsen: Heat Recovery from Aluminium Reduction Cells, *Light Metals 2011*, 393-398.
4. A. Arkhipov, I. Necheporenko, A. Mukhanov, N. Ahli, and K AlMarzooqi: Modelling Study of Exhaust Rate Impact on Heat Loss from Aluminium Reduction Cells, *Light Metals 2019*, 625-635.
5. T.A. Aarhaug and A.P. Ratvik: Aluminium Primary Production Off-Gas Composition and Emissions: An Overview, *JOM* (2019), https://doi.org/10.1007/s11837-019-03370-6
6. NIST-JANAF Thermochemical Tables, https://janaf.nist.gov/
7. A. Solheim: Current Efficiency in Aluminium Reduction Cells: Theories, Models, Concepts, and Speculations, *Light Metals 2014,* 753-758.
8. T.G. Pearson and J. Waddington: Electrode Reactions in the Aluminium Reduction Cell, *Discuss. Farad. Soc.* **1** 307-320 (1947).
9. W. Haupin and H. Kvande: Mathematical Model of Fluoride Evolution from Hall-Héroult Cells, *Light Metals 1993*, 257-263.
10. A. Solheim and Å. Sterten: Activity of Alumina in the System NaF-AlF_3-Al_2O_3 at NaF/AlF_3 Molar Ratios Ranging from 1.4 to 3, *Light Metals 1999*, 445-452.
11. A. Solheim, S. Rolseth, E. Skybakmoen, L. Støen, Å. Sterten, and T. Støre: Liquidus Temperatures for Primary Crystallization of Cryolite in Molten Salt Systems of Interest for the Aluminium Electrolysis, *Met. Trans. B* **27B** 739-744 (1996).
12. J. Thonstad, P. Fellner, G.M. Haarberg, J. Hives, H. Kvandem and Å. Sterten: Aluminium Electrolysis, 3rd Edition, Aluminium-Verlag, 2001.
13. I.A. Zlochower: Experimental Flammability Limits and Associated Theoretical Flame Temperatures as a Tool for Predicting the Temperature Dependence of these Limits, *J. Loss Prev. Process Ind.* **25**(3) 555-560 (2012).
14. F.H. Verhoff and J.T. Banchero: Predicting Dew Points of Flue Gases, *Chem. Eng. Prog.*, **70**(8) 71-72 (1974).
15. A.G. Okkes and B.V. Badger: Get Acid Dew Points of Flue Gas, *Hydrocarbon Proc.*, **66**(7) 53-55 (1987).
16. R.R. Pierce, Estimating Acid Dewpoints in Stack Gases, *Chemical Engineering*, **84**(8) 125-128 (1977).
17. O.-A. Lorentsen, A. Dyrøy, and M. Karlsen: Handling CO_{2eq} from an Aluminum Electrolysis Cell, *Light Metals 2009*, 263-268.
18. Thor A. Arhaug, SINTEF, personal communication (2015).